Lipid Clustering in Bilayers Detected by the Fluorescence Kinetics and Anisotropy of *trans*-Parinaric Acid

C. Reyes Mateo,*‡ Jean-Claude Brochon,* M. Pilar Lillo,‡ and A. Ulises Acuña‡

*Laboratoire pour l'Utilisation du Rayonnement Electromagnétique, Centre National de la Recherche Scientifique-Ministère de l'Education Nationale-Commissariat à l'Energie Atomique, Bâtiment 209D, Université Paris Sud, F-91405 Orsay, France, and ‡Instituto de Quimica-Fisica "Rocasolano," CSIC, Serrano 119, E-28006 Madrid, Spain

ABSTRACT This work confirms the ability of the fluorescent probe *trans*-parinaric acid to detect gel/fluid heterogeneity in lipid bilayers and shows a simple and useful method to quantify this heterogeneity. Taking advantage of the maximum entropy method, we have resolved the probe fluorescence lifetime distributions in homogeneous solutions and in single and two-component lipid bilayers at different temperatures. A precise description of the emission kinetics was obtained as a function of viscosity in the homogeneous solution and as a function of the phase composition (gel/fluid) in the lipid bilayers. These data show, unambiguously, that the same distribution pattern, with two well resolved lifetime classes, is observed both in pure solvents and in fluid bilayers. This distribution is modified during the thermotropic phase transition, with the appearance of a long lifetime component. The anisotropy experiments confirm that the amplitude of this component is proportional to the fraction of probe located in the gel phase. From this fraction we have quantified the amount of gel phase in the binary bilayer system dimyristoyl phosphatidylcholine/dipalmitoyl phosphatidylcholine and determined the thermotropic phase diagram of the mixture. This phase diagram agrees well with that calculated assuming ideal mixing of the lipids (Marbrey, S., and J. M. Sturtevant. 1976. *Proc. Natl. Acad. Sci. USA.* 73:862–3866).

INTRODUCTION

The lipid component of biological membranes has been usually visualized as a physically homogeneous system. However, there is growing evidence in recent works that lipid domains of different structure and composition might exist in biological membranes, even at physiological temperatures (Ho et al., 1992; Mateo et al., 1991; Illsley et al., 1988; Gordon et al., 1983; Schroeder et al., 1983). Since these domains introduce in the bilayer a source of lateral heterogeneity, they may play an important role in the support and modulation of membrane protein functions (Aloia et al., 1988). Alteration of temperature or lipid composition at atmospheric pressure can lead to changes in the domain structure and, thereby, in the functional state of the cell.

The experimental demonstration of this heterogeneity at a molecular level is of a great interest in current membrane research and is being pursued by means of several spectroscopic techniques (reviewed by Devaux et al. (1985)). Among those, the methods based on fluorescence detection present the advantages of high sensitivity, time resolution, and multiplicity of signals (Van der Meer et al., 1988). Events on time scales ranging from 0.1 μs to picoseconds are observable using the fluorescence signal. In many of these methods, a lipophilic fluorescent probe is introduced into the lipid bilayer and a number of spectral parameters are monitored (Lentz et al., 1989). These spectroscopic parameters are, frequently, sensitive to the lipid environment surrounding the fluorophore. A variety of probes have been used to detect membrane heterogeneity (Ho et al., 1992; Parasassi et al., 1991a; Ruggiero and Hudson, 1989a; Davenport et al., 1988; Fiorini et al., 1988; Bultmann et al., 1991). Thus, the high spectral sensitivity of the Laurdan molecule to the phase state of phospholipids has been recently used to detect and quantify lipid phases in phospholipid vesicles (Parasassi et al., 1990, 1991a). Similarly, since the fluorescence parameters of diphenylhexatriene, DPH, are weakly sensitive to the fluidity of its microenvironment (Barrow and Lentz, 1985) this probe has also occasionally been used to investigate the presence of gel domains in bilayers (Ho et al., 1992; Fiorini et al., 1988).

trans-Parinaric acid, *t*-PnA, a fluorescent polyene fatty acid probe (Sklar et al., 1977b), has been used to detect lateral heterogeneity in several occasions (Mateo et al., 1991; Ruggiero and Hudson, 1989b). In this case, the detection of heterogeneity in lipid bilayers is based on the high sensitivity of the probe fluorescence kinetic to lipid local density (Sklar et al., 1977b; Hudson et al., 1986). The investigation of lipid clustering using *t*-PnA is possible if the multiple components of the fluorescence decay are correctly assigned to distinct fractions of the bilayer. However, it has been reported (Parasassi et al., 1984) that changes in the photophysical parameters of *t*-PnA resembling those recorded in heterogeneous lipid bilayers could be also observed in homogeneous solvents, where no association of solvent molecules is obviously expected. Therefore, the utility of this probe in the detection of lipid domains has been seriously questioned.

The most important outcome of the present work is the experimental confirmation that the fluorescence kinetics of *t*-PnA can indeed be used to detect and quantify in a simple way the coexistence of ordered and disordered phases in lipid bilayers. With this purpose, the fluorescence parameters

Received for publication 4 June 1993 and in final form 5 August 1993.

Address reprint requests to J.-C. Brochon.

0006-3495/93/11/2237/11 $2.00

(lifetime and anisotropy) of *t*-PnA have been determined, at different temperatures, in isotropic solvents of different viscosity and in well characterized heterogeneous lipid bilayers. Since *t*-PnA is not very soluble in organic solvents, a detailed study of the effect of solvent viscosity on the *t*-PnA fluorescence had not been carried out until now. The results show that fluorescence decays of the probe in pure solvents and in lipid bilayers at temperatures well above the transition temperature are described by a bimodal fluorescence lifetime distribution. An abrupt change in this bimodal distribution is observed during the phase transition with the appearance of a new lifetime component centered to higher values. This component corresponds to the emission of the probe located in the gel phase, and its amplitude is proportional to the fraction of probe in this phase. Structural properties (order parameters) of the gel and fluid phases have been derived from the heterogeneous anisotropy decay of the probe in the temperature range where the two distinct environments coexist.

EXPERIMENTAL PROCEDURES

Materials

trans-Parinaric acid, *t*-PnA, was obtained from Molecular Probes (Eugene, OR) and was purified by recrystallization from hexane. Purity was controlled by both absorption and emission spectroscopy and high-performance liquid chromatography. Paraffin oil (PRIMOL ESSO 353), used without further purification, was free of fluorescent impurities in the wavelength range of interest. Dipalmitoyl phosphatidylcholine (DPPC) and dimyristoyl phosphatidylcholine (DMPC) were obtained from Serdary (London, Ontario, Canada) and palmitoyloleoyl phosphatidylcholine (POPC) from Sigma Chemical Co. (St Louis, MO). These lipids were used as supplied. Stock solutions of *t*-PnA were prepared in ethanol, vigorously bubbled with nitrogen, and stored in the dark at −20°C before use.

Methods

Unilamellar vesicles

Multilamellar vesicles were prepared by resuspending the appropriate amounts of the dried lipid in phosphate buffer (pH 7), the suspension was then heated above the phase transition and vortexed. Large unilamellar vesicles, with a mean diameter of 90 nm, were prepared from the multilamellar vesicles by extrusion techniques, through Nucleopore filters with 100 nm pore size, as previously described (Hope et al., 1985). The lipid mixtures were prepared by dissolving the weighted components in a small volume of chloroform and evaporating the solvent under nitrogen.

Incorporation of the t-PnA probe

To prepare the paraffin oil samples, aliquots of the stock solution were deposited on the walls of a test tube and evaporating the ethanol solvant by blowing a stream of nitrogen. Then paraffin oil was added to the tube and the mixture stirred at 40°C to obtain a 10^{-6} M homogeneous solution of the probe. In the bilayer samples, *t*-PnA was added from the stock solution directly into the lipid dispersion which was then vigorously bubbled with nitrogen. The samples were stirred and heated above the phase transition temperature to facilitate the incorporation of probe into the bilayers. The probe/lipid molar ratio was 1/200 phospholipids. Samples were measured immediately after preparation.

Fluorescence measurements

The fluorescence intensity decay and time-resolved anisotropy were obtained by recording the two polarized components $Ivv(t)$ and $Ivh(t)$, using the time-correlated single photon counting technique. The excitation pulse source was the synchrotron radiation emitted by the positron storage ring of Orsay working at a frequency of 8.33 MHz in the two-bunch mode. The storage ring provides a light pulse with a full width at half maximum of ≈500 ps. Two JY 25 monochromators were used to select the excitation (304 nm, 322 nm, $\Delta\lambda = 6$ nm) and detection (405 nm, $\Delta\lambda = 8$ nm) wavelengths; the detector was a microchannel plate Hamamatsu R1564U, Hamamatsu Photonic K.K. (Hamamatsu City 431-32, Japan). The apparatus response function to the excitation pulse was measured with a scattering ludox solution at the emission wavelength, alternatively with the two components of the polarized fluorescence decay. Time resolution were either 18, 35, or 75 ps per channel. Either 1024 or 2048 channels were used to store the decays. Some of the experiments were carried out using a picosecond laser system as excitation source. The apparatus consisted of a mode-locked, cavity-dumped dye laser system (dye, Rh6G) synchronously pumped by an Ar^+ laser, providing 10–15-ps pulses at 800 kHz. Using a double harmonic generator samples, were excited at 300 nm and emitted photons were detected at 405 nm by a microchannel plate photomultiplier (Hamamatsu R1564U). The instrumental response function was 80–100 ps. Further details of the laser spectrometer have been published elsewhere (Moya et al., 1986).

METHODS OF DATA ANALYSIS

The analysis of total fluorescence intensity $I(t)$ and fluorescence anisotropy $r(t)$ was performed by the Maximum Entropy Method (MEM), for which the fluorescence lifetime τ_i and rotational correlation time θ_i components are equally spaced in logarithmic scale (Livesey and Brochon, 1987; Brochon and Livesey, 1988; Brochon et al., 1992).

The principles of MEM as applied to time-resolved fluorescence are outlined in the following. With a vertically polarized exciting pulse, the paralell $Ivv(t)$ and perpendicular $Ivh(t)$ components of the fluorescence intensity at time t after the start of the excitation are:

$$Ivv(t) = \frac{1}{3}E_\lambda(t)*\left[\int_0^\infty\int_0^\infty\int_{-0.2}^{0.4}\gamma(\tau,\theta,r_0)e^{-t/\tau}(1+2r_0e^{-t/\theta})\,d\tau\,d\theta\,dr_0\right] \quad (1)$$

$$Ivh(t) = \frac{1}{3}E_\lambda(t)*\left[\int_0^\infty\int_0^\infty\int_{-0.2}^{0.4}\gamma(\tau,\theta,r_0)e^{-t/\tau}(1-r_0e^{-t/\theta})\,d\tau\,d\theta\,dr_0\right] \quad (2)$$

where $E_\lambda(t)$ is the temporal shape of the excitation flash, * denotes a convolution product, and $\gamma(\tau,\theta,r_0)$ represents the number of fluorophores with fluorescence lifetime τ, rotational correlation time θ, and initial anisotropy r_0.

If all the emitting species are assumed to display the same initial anisotropy and rotational dynamics, Eqs. 1 and 2 can be rewritten as:

$$Ivv(t) = \frac{1}{3}E_\lambda(t)*\left[\int_0^\infty\alpha(\tau)e^{-t/\tau}\,d\tau\left(1+2\int_0^\infty\rho(\theta)e^{-t/\theta}\,d\theta\right)\right] \quad (3)$$

$$Ivh(t) = \frac{1}{3}E\lambda(t)*\left[\int_0^\infty\alpha(\tau)e^{-t/\tau}\,d\tau\left(1-\int_0^\infty\rho(\theta)e^{-t/\theta}\,d\theta\right)\right] \quad (4)$$

and

$$r_0 = \int_0^\infty\rho(\theta)\,d\theta$$

where $\alpha(\tau)$ and $\rho(\theta)$ are, respectively, the distribution functions of the fluorescence lifetimes and the rotational correlation times. The $\alpha(\tau)$ profile is given from an initial analysis of the total fluorescence intensity.

The expression for the total fluorescence intensity, $I(t)$, can be obtained by summing the parallel and perpendicular components:

$$I(t) = Ivv(t) + 2Ivh(t) = E_\lambda(t)^* \int_0^\infty \alpha(\tau) e^{-t/\tau}\, d\tau \qquad (5)$$

$I(t)$ can also be recorded in one experiment by setting the polarizer at the "magic" angle (54.75°).

Since the experimental data are noisy and finite in extent, there is strictly an infinite set of $\alpha(\tau)$ and $\rho(\theta)$ solutions within the experimental error. One may select the distribution that maximizes the Skilling-Jaynes entropy S (Jaynes, 1983; Livesey and Skilling, 1985). For the total intensity, this entropy is given by:

$$S = \int_0^\infty \left[\alpha(\tau) - m(\tau) - \alpha(\tau) \log \frac{\alpha(\tau)}{m(\tau)} \right] d\tau \qquad (6)$$

while for the anisotropy is defined as:

$$S = \int_0^\infty \left[\rho(\theta) - m(\theta) - \rho(\tau) \log \frac{\rho(\theta)}{m(\theta)} \right] d\theta \qquad (7)$$

where m is our prior knowledge about the lifetime distribution; it should be flat in $\log \tau$ and $\log \rho$ if there is no information about it before measurement.

In order to ensure that the recovered distribution agrees with the experimental data, we chose to bound the feasible set by a chi-squared statistic:

$$\sum_{k=1}^{M} \frac{(I_{k,vv}^{\text{calc}} - I_{k,vv}^{\text{obs}})^2}{\sigma_{k,vv}^2} + \sum_{k=1}^{M} \frac{(I_{k,vh}^{\text{calc}} - I_{k,vh}^{\text{obs}})^2}{\sigma_{k,vh}^2} \leq 2M \qquad (8)$$

where I^{calc}, I^{obs} are the calculated and observed intensities, σ_k^2 is the variance of the kth point, and M is the total number of points in each component.

The center τ_j of a single class j of lifetimes over the $\alpha(\tau_i)$ distribution is defined as:

$$\tau_j = \frac{\sum_i \alpha(\tau_i)\tau_i}{\sum_i \alpha_i(\tau_i)} \qquad (9)$$

and the center of a correlation time distribution is calculated as:

$$\theta_j = \frac{\sum_i \rho(\theta_i)\theta_i}{\sum_i \rho_i(\theta_i)} \qquad (10)$$

the summation being performed on the significant values of $\alpha(\tau_i)$ and $\rho(\theta_i)$ for the j class. The fractional areas c_i and β_j are, respectively, the ratio of areas of the $\sum \alpha(\tau_i)$ and $\sum \rho(\theta_i)$ peaks to that of the entire surface of the distribution. In this study the analysis were performed starting with 100 lifetimes (from 0.1 to 50 or 100 ns) and 100 correlation times (between 0.1 and 100 ns).

When the probe is assumed to be located in two different environments, the fluorescence anisotropy decay was analyzed using a Marquardt nonlinear least squares search, by fitting simultaneously the horizontal and vertical fluorescence decay traces (Cross and Flemming, 1984). The anisotropy data were fit to an "associative" model (Ruggiero and Hudson, 1989b; Mateo et al., 1991) in which the lifetime parameters of the total intensity decay are specifically associated with individual anisotropy parameters. The corresponding model accounts for the possibility of a probe being localized in two different environments S and F. The corresponding species have independent fluorescence, $I_n(t)$, and anisotropy, $r_n(t)$, decays (with n = S or F). The total fluorescence decay, $I(t)$, is given by a linear combination of the kinetic parameters of the two emitting species:

$$I(t) = \sum_{n=S,F} a_n I_n(t) \qquad \sum_{n=S,F} a_n = 1 \qquad (11)$$

The time-dependent fraction of the total light emitted by the probe molecules localized in the environment n is given by:

$$f_n(t) = a_n \frac{I_n(t)}{I(t)} \qquad (12)$$

The individual fluorescence decay, $I_n(t)$ in Eq. 11 is often described by a single exponential function. However, most of the dyes embedded in bilayers show a multicomponent fluorescence decay. Then, a general expression for $I_n(t)$ could be:

$$I_n(t) = \sum_{j=1}^{m} c_{nj} \exp(-t/\tau_{nj}) \qquad \left(\sum_{j=1}^{m} c_{nj} = 1 \right) \qquad (13)$$

Using Eqs. 11 and 13, the time-dependent fluorescence fraction $fn(t)$ is:

$$f_n(t) a_n \frac{\sum_{j=1}^{m} c_{nj} \exp(-t/\tau_{nj})}{\sum_{n=S,F} a_n \sum_{j=1}^{m} c_{nj} \exp(-t/\tau_{nj})} \qquad (14)$$

Since at time zero $f_n(0) = a_n$, the weighting factors a_n may be derived from the parameters of the fluorescence decay. If the radiative lifetime and absorption coefficient of the probe are not very different in the two environments, a_n represents the molar fraction of the probe in each environment ($a_n = \chi_p^n$).

In an heterogeneous system, the fluorescence anisotropy decay $r(t)$ is a linear combination of the anisotropy decay of each emitting species:

$$r(t) = \sum_{n=S,F} f_n(t) r_n(t) \qquad (15)$$

To reduce the number of adjustable parameters in the numerical analysis, the anisotropy function of each dye population was represented by a single rotational correlation time θ and a residual anisotropy r_∞ (the cone model):

$$r_n(t) = \beta_n \exp(-t/\theta_n) + r_{\infty n} \qquad \beta_n + r_{\infty n} = r_n(0) \qquad (16)$$

The anisotropy at $t = 0$, $r_n(0)$ was assumed to be the same for the two populations and was not fixed (Ruggiero and Hudson, 1989b).

If the fraction of the probe localized in a specific phase (χ_p^n) and the partition coefficient of the probe between the gel and fluid phases ($K_p^{S/F}$) are known, it is possible to quantify the fraction of gel phase χ^S from the expression:

$$K_p^{S/F} = \frac{\chi_p^S/\chi^S}{\chi_p^F/\chi^F} \qquad (\chi^S + \chi^F = 1) \qquad (17)$$

RESULTS

Fluorescence intensity decay kinetics

Isotropic solutions

The fluorescence kinetics of *t*-PnA was studied in isotropic solvents (ethanol, cyclohexane, and paraffin oil) at temperatures from 10° to 50°C. In the three solvents the *t*-PnA fluorescence was well fitted by two-lifetimes decay functions (Fig. 1 and Table 1). In some cases, a third long lifetime component was observed, with a contribution of less than 1% and was calculated as artefactual. The relative amplitude of the long lifetime component, τ_L, accounts for almost 80% of the total distribution area. Changing solvent polarity, viscosity or temperature does not modify the bimodal lifetime distribution and only the center location of the lifetime peaks is varied. The Arrhenius plot of the long lifetime component τ_L (Fig. 2) shows that in the three solvents log τ_L increases linearly with $1/T$. For a constant temperature the value of τ_L was found to be larger in the solvent with higher viscosity.

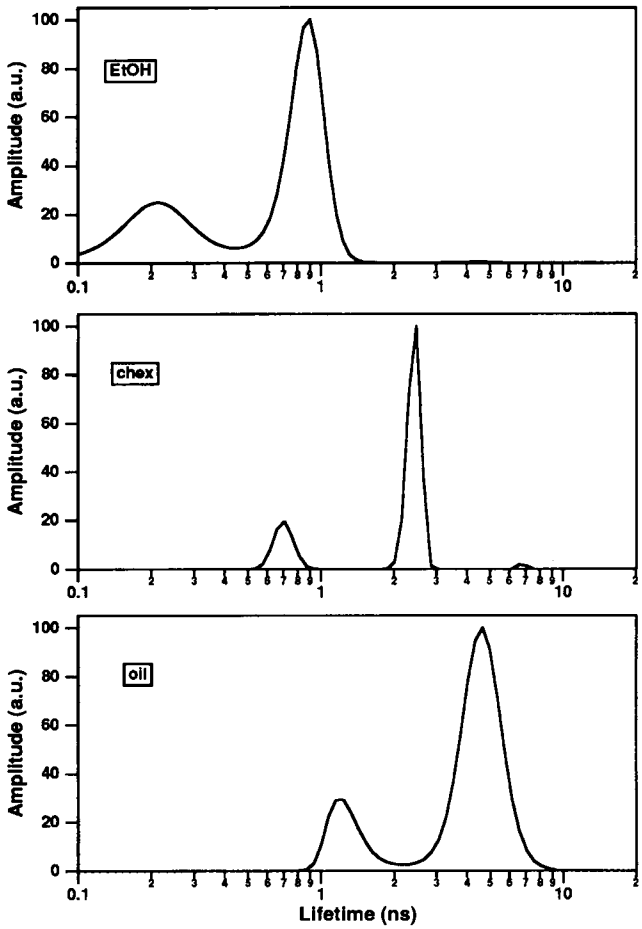

FIGURE 1 Fluorescence lifetime distributions of *t*-PnA in ethanol, cyclohexane, and paraffin oil at 20°C as recovered by MEM.

Single-component lipid bilayers

Fluid phase—In the fluid phase of the saturated phospholipids, DPPC (T_m = 42°C) and DMPC (T_m = 23°C), the fluorescence decay of *t*-PnA is well described by a bimodal lifetime distribution, similar to that observed in the paraffin oil (Table 1). The same distribution pattern was recorded in the fluid phase of the unsaturated phospholipid POPC (T_m = −5°C), at temperatures above 20°C (Table 2 and Fig. 3). The Arrhenius plot of the long lifetime component in the three lipid systems (Fig. 2) shows that, also in this case, log τ_L increases linearly with $1/T$, as in isotropic solvents. For a constant temperature τ_L was found to be larger in the phospholipids with a higher transition temperature.

In the case of POPC at temperatures below 20°C the distribution pattern corresponding to the short lifetime broadened when temperature was decreasing and finally, it was split in two new lifetime components (Fig. 3 and Table 2).

Gel phase—The change in the lifetime distribution of *t*-PnA through the lipid phase transition is shown in Fig. 4. In DPPC there is an abrupt change in the distribution pattern at 42°C, with the appearance of a new lifetime component centered at 20 ns (Table 1). This pattern was preserved at lower temperatures and the only change observed was a shift to longer lifetime values. Similar changes were detected in DMPC through the lipid phase transition (Table 1).

Two-component lipid bilayers

The fluorescence intensity decay of *t*-PnA was measured in large unilamellar vesicles made up with an equimolar mixture of DMPC/DPPC in the temperature range between 25° and 45°C. The lifetime distributions and fit parameters are shown in Fig. 5 and Table 3, respectively. The thermal phase diagram of this mixture, previously determined by differential scanning calorimetry (Mabrey and Sturtevant, 1976), provides information on a system of coexisting gel/fluid phases located in the range of physiological temperatures (see Fig. 7). In the temperature range from 25° to 33°C, the fluorescence lifetime distribution is similar to that recorded in the gel phase of DPPC. From 34° to 37°C, the contribution of the long lifetime component decreases and finally a bimodal distribution is obtained from 38°C to higher temperatures (Fig. 5).

Similar experiments were carried out in DMPC/DPPC mixtures containing 0.7 mol fraction of DMPC. The fluorescence parameters are shown in Table 3. The amplitude of the long lifetime component decreases from 30° to 34°C.

Time-resolved fluorescence anisotropy decay measurements

Isotropic solvents

In ethanol and cyclohexane the anisotropy decay of the probe was satisfactorily fitted to a single correlation distribution function (Table 4). The measured $r(0) = \sum \beta_i$ is lower than the expected value r_0 = 0.4 (Shang et al., 1991), probably due to very fast correlation processes of the probe which cannot be resolved with our instrument. In paraffin oil the fluorescence anisotropy decay of *t*-PnA was described by three rotational correlation times (Table 4). The values of these rotational correlation times decrease with rising the temperature, although their relative weights remain approximately constant. Above 20°C the first correlation time θ_1 becomes too fast to be resolved by our instrumentation.

Lipid bilayers

The fluorescence anisotropy of *t*-PnA in single-component lipid bilayers, in both gel and fluid phases, decays in fractions of nanoseconds to a residual anisotropy r_∞. This limiting value can be related to the second rank order parameter, $\langle P_2 \rangle$, of the acyl chain distribution (Van der Meer et al., 1984). The corresponding fit parameters of the curves are shown in Table 5 as a function of temperature. In the gel phase the rotational correlation time is so fast that could not be quantified in several cases. The fluorescence anisotropy decay of the probe at the transition temperature shows an anomalous behavior, as noted before by Wolber and Hudson (1981) and Ruggiero and Hudson (1989b), with a very fast decay to a minimal value and a subsequent increase. The upward cur-

TABLE 1 Fluorescence intensity decay parameters, recovered by MEM, of *t*-PnA in homogeneous solution and in large unilamellar vesicles of DMPC and DPPC as a function of temperature

Sample	T/°C	C_1	τ_1/ns	C_2	τ_2/ns	C_3	τ_3/ns
EtOH	10	0.29	0.3	0.71	1.1		
	20	0.34	0.3	0.66	0.9		
	30	0.29	0.3	0.71	0.7		
Cyclohex.	10	0.15	0.9	0.85	2.7		
	20	0.18	0.9	0.82	2.3		
	50	0.12	0.7	0.88	1.3		
Paraffin oil	10	0.28	1.6	0.72	5.9		
	13	0.20	1.7	0.80	5.4		
	15	0.22	1.6	0.78	5.1		
	20	0.15	1.4	0.85	4.3		
	32	0.17	1.0	0.83	3.0		
	35	0.23	0.9	0.77	2.7		
	42	0.14	0.7	0.86	2.2		
	50	0.10	0.6	0.90	1.9		
DPPC	10	0.11	1.3	0.06	7.6	0.83	45
	20	0.11	1.0	0.14	9.0	0.75	37
	25	0.11	1.5	0.10	9.1	0.79	35
	30	0.11	1.7	0.07	5.7	0.82	30
	32	0.11	0.9	0.11	5.6	0.78	26
	41	0.15	1.3	0.43	5.0	0.42	29
	42	0.24	0.9	0.51	4.3	0.25	20
	50	0.26	0.7	0.71	2.8	0.03	19
DMPC	13	0.17	1.3	0.18	10.0	0.65	29
	15	0.22	1.0	0.23	4.7	0.55	22
	22	0.26	2.1	0.24	5.0	0.50	20
	23	0.27	1.1	0.32	4.4	0.41	20
	25	0.24	1.4	0.40	6.0	0.36	15
	30	0.38	1.4	0.62	5.5		
	35	0.18	1.1	0.82	4.2		
	40	0.30	1.1	0.70	3.5		

C_i and τ_i are the integrated relative amplitude and center value, respectively, of each lifetime class. C_i, ±0.04; τ_1, ±0.3, τ_2, ±0.8, τ_3, ±2.0 ns.

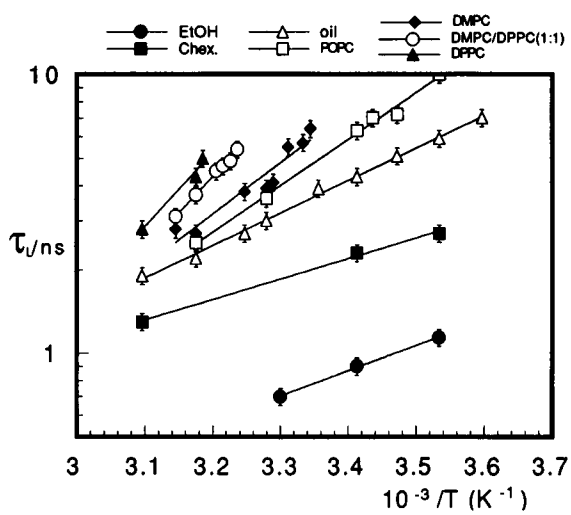

FIGURE 2 Arrhenius plot of the long lifetime component (τ_L) of the fluorescence distribution of *t*-PnA in ethanol, cyclohexane, and paraffin oil and in large unilamellar vesicles of POPC, DMPC, DPPC/DMPC (1:1), and DPPC.

TABLE 2 Fluorescence intensity decay parameters, recovered by MEM, of *t*-PnA in large unilamellar vesicles of POPC

Sample	T/°C	C_1	τ_1/ns	C_2	τ_2/ns	C_3	τ_3/ns
POPC	10	0.16	0.7	0.31	2.2	0.53	9.0
	15	0.18	0.8	0.28	2.0	0.54	7.4
	20	0.24	0.8	0.21	1.9	0.55	6.1
	30	0.37	1.0			0.63	4.2
	32	0.33	1.1			0.67	3.6
	40	0.31	0.8			0.69	3.0
	42	0.18	0.8			0.82	2.5
	50	0.28	0.6			0.72	2.3

C_i and τ_i are the integrated relative amplitude and barycenter value, respectively, of each lifetime class. C_i, ±0.04; τ_1, ±0.2, τ_2, ±0.3, τ_3, ±1.0 ns.

vature in $r(t)$ is a strong indication of rotational heterogeneity associated with different fluorescence lifetime components (Ludescher et al., 1987). These curves were analyzed with the associative model described above, by assuming the presence of two subpopulations of the probe localized in two differents phases. The longer lifetime component of the distribution was associated with the fraction of probe localized in the gel phase, while the short components were associated with the probe molecules embedded in the fluid phase. Anisotropy parameters from analysis are given in Table 5.

In the equimolar mixture DMPC/DPPC at temperatures above 39° and below 34°C the anisotropy decays could be described by a single rotational correlation time and a constant anisotropy value as it was observed, respectively, in the fluid and gel phases of single-component lipid bilayers (Table 5 and Fig. 6). In the 34–38°C range the anisotropy decay shows the upward curvature observed in single-component lipid bilayers near the phase transition (Fig. 6). The anisotropy decay of *t*-PnA in DMPC/DPPC lipid bilay-

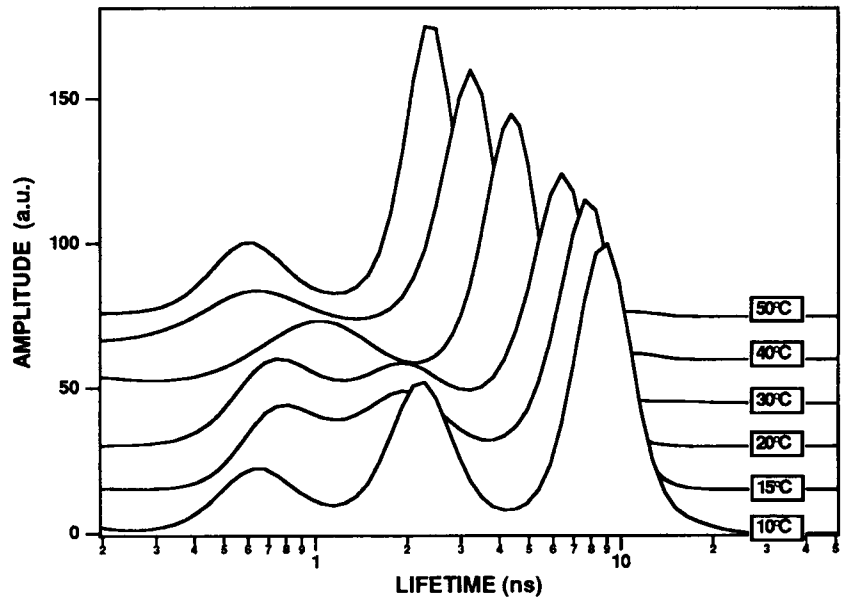

FIGURE 3 The fluorescence lifetime distribution of *t*-PnA in POPC as a function of temperature.

ers with a different composition (7:3 molar ratio) in the temperature range of 31–34°C was identical to that observed in the equimolar bilayers (see Table 5). The two subpopulations of probe molecules are characterized by quite different residual anisotropy values (r_∞^S and r_∞^F) and rotational correlation times, θ_S and θ_F. The residual anisotropy r_∞^S is similar to the value measured in the gel phase of the single-component lipid bilayer. The value for fluid environment, r_∞^F, is also typical of the fluid phases of DMPC and DPPC.

DISCUSSION

Isotropic solvents

The main limitation in the use of *t*-PnA to detect lipid domains has been the intrinsic heterogeneity of its fluorescence decay in isotropic solvents. Here we confirm that the probe exhibits in fluid solvents, in the range of temperatures and viscosities studied, two well defined lifetime components. Our results reproduce, in the most of the cases, what has been observed by Ruggiero and Hudson (1989a) using pulse light technique and assuming discrete lifetimes. On the contrary, the results are not in agreement with those found by Parasassi et al. (1984) using multifrequency phase technique and discrete lifetimes, although could be well compared with those obtained using the same technique but assuming a continuous lifetime distribution (Conti and Parasassi, 1987). The origin of the multiexponential decay could be explained, as a first hypothesis, assuming a two-excited-state model, as for DPH (Parasassi et al., 1991b). *t*-PnA present two closely spaced excited states (Sklar et al., 1977a; Hudson and Kohler, 1973). After excitation to the allowed excited state S2, there is a rapid interconversion to the lower excited state S1, and most

TABLE 3 Fluorescence intensity decay parameters, recovered by MEM, of *t*-PnA in LUVs containing lipid mixtures of DMPC/DPPC

DMPC/DPPC molar ratio	*T*/°C	C_1	τ_1/ns	C_2	τ_2/ns	C_3	τ_3/ns
1:1	25	0.15	1.4	0.24	8.3	0.61	28
	30	0.15	1.7	0.27	8.1	0.58	26
	33	0.17	1.5	0.25	6.4	0.58	24
	34	0.16	1.3	0.32	5.8	0.52	24
	35	0.21	1.4	0.38	5.7	0.41	23
	36	0.21	1.4	0.50	5.3	0.29	22
	37	0.17	1.1	0.69	4.9	0.14	22
	38	0.28	1.3	0.62	4.7	0.10	21
	39	0.26	1.2	0.71	4.5	0.03	19
	42	0.28	1.1	0.70	3.7	0.02	16
	45	0.30	0.9	0.70	3.1		
7:3	29	0.18	1.1	0.17	4.0	0.65	21
	30	0.17	1.8	0.26	6.4	0.57	22
	31	0.16	1.5	0.40	6.0	0.44	22
	32	0.24	1.3	0.55	5.2	0.21	17
	33	0.24	1.3	0.66	5.3	0.10	17
	34	0.28	1.3	0.69	5.2	0.03	21

C_i and τ_i are the integrated relative amplitude and center value, respectively, of each lifetime class. C_i, ±0.04; τ_1, ±0.02, τ_2, ±0.8, τ_3, ±2.0 ns.

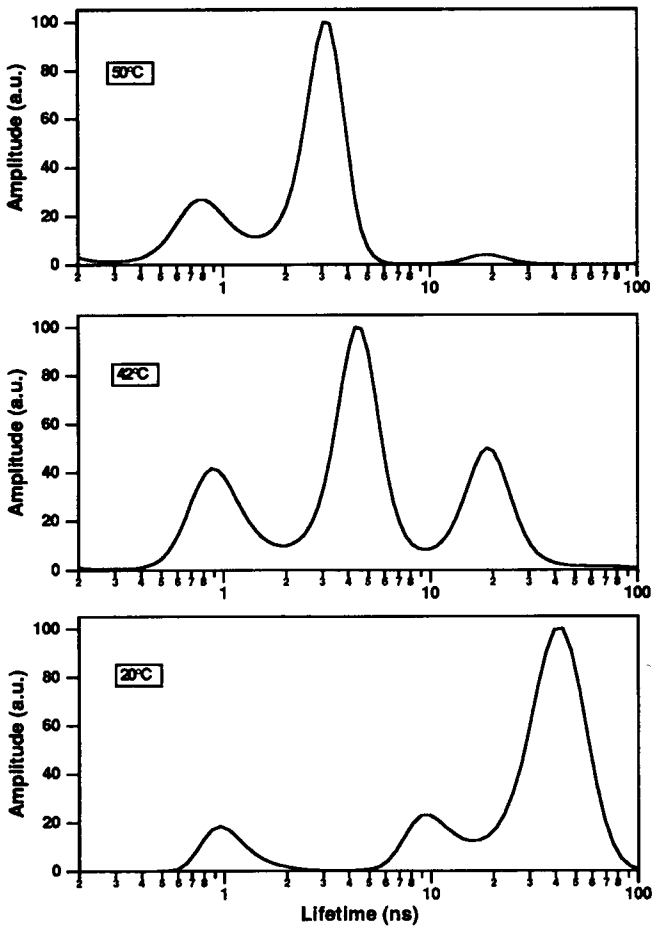

FIGURE 4 Effect of the lipid phase transition on the fluorescence lifetime distribution of *t*-PnA incorporated in DPPC large unilamellar vesicles (T_m = 42°C).

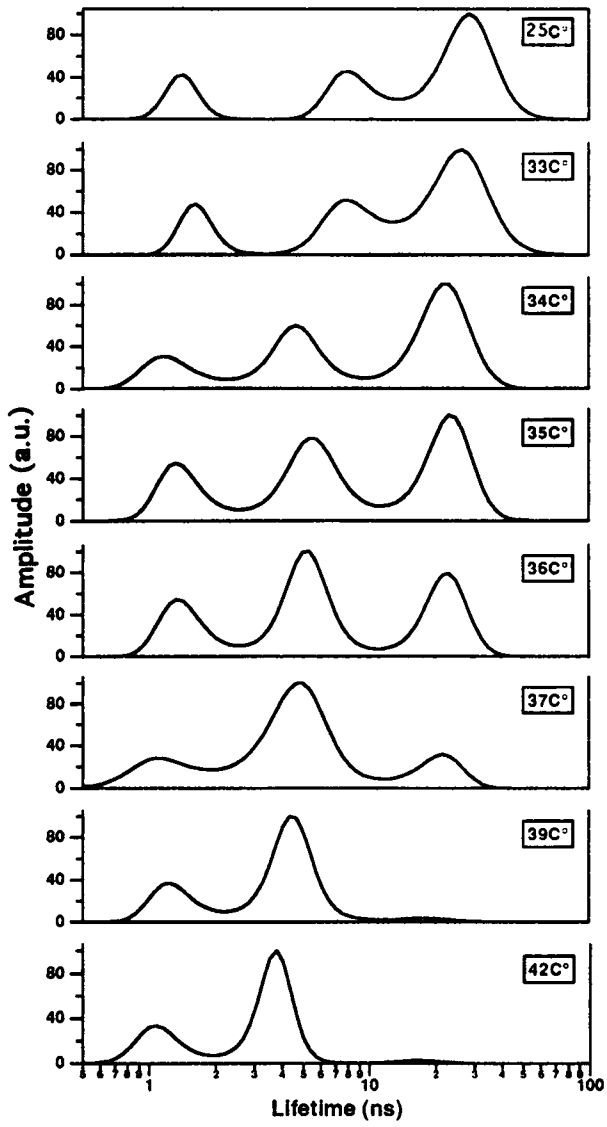

FIGURE 5 The fluorescence lifetime distribution of *t*-PnA incorporated in an equimolar mixture of DPPC/DMPC as a function of temperature.

of the emission occurs from this state. The result is that the fluorescence lifetimes observed reflect both the intrinsic decay rates from S1 and S2 and the interchange rates between the two excited states. The excited probe interacts with the solvent molecules, and the different exchange kinetics between the solvating shells influence the interchange rates of these excited states giving rise to a broad lifetime distribution. Hudson et al. (1986) has also suggested that the multiexponential decay of the probe is due to a photochemical process leading to several emitting excited-state conformers that may thermally revert to the all-*trans* form on returning to the ground state. The certain is that the exact origin of this behavior is not yet clear. However, for the objective of the present work, the most important feature is the observation of a biexponential fluorescence kinetics which is preserved in the temperature range of interest for membrane research.

In simple alkane solvents as cyclohexane or paraffin oil, the lifetime values observed for *t*-PnA are a function of polarizability and temperature. The temperature effects on the *t*-PnA fluorescence was previously observed (Sklar et al., 1977a) and is confirmed here (Fig. 2). These results are compared with those obtained by Ruggiero et al. (1989a) in squalene. In paraffin oil the temperature dependence of the longest lifetime component is stronger than in squalene. In cyclohexane, increasing temperature affects, slightly, the fluorescence parameters of the probe. Activation energies, determined for paraffin oil, squalene, and cyclohexane are 5.3 ± 0.2, 4.6 ± 0.9, and 3.4 ± 0.2 kcal/mol, respectively. At 13°C the respective viscosity of these solvents is η^{oil} = 289 cP, η^{squal} = 44 cP, and η^{chex} = 0.7 cP. Therefore, changes in the temperature will have a major effect on the *t*-PnA lifetimes if the solvent is viscous. Since the radiative lifetime of *t*-PnA can be considered rather constant for a variety of solvents and over the temperature range of 12° to 66°C (Sklar et al., 1977a), it is possible to assume that changes observed in the fluorescence lifetime of the probe are due to changes in its radiationless decay rate. Therefore, the radiationless process will be activated not only by increasing temperature but also by decreasing viscosity. This behavior attributed to changes in viscosity could be only due

TABLE 4 Fluorescence anisotropy parameters, recovered by MEM, of *t*-PnA in homogeneous solution

Solvent	T/°C	β_1	θ_1/ns	β_2	θ_2/ns	β_3	θ_3/ns
Paraffin oil	5	0.04	0.2	0.06	3.6	0.30	37.0
	13	0.06	0.2	0.08	2.5	0.26	19.0
	20	0.07	0.2	0.07	2.1	0.23	9.0
	32			0.08	1.1	0.23	5.0
	35			0.09	1.1	0.21	4.6
	42			0.06	0.8	0.27	2.2
	50			0.04	0.3	0.24	1.8
Cyclohexene	10	0.14	0.3				
	20	0.11	0.2				
	50	0.18	0.1				
Ethanol	10	0.23	0.3				
	20	0.22	0.2				
	30	0.32	0.1				

θ_i and β_i are the rotational correlation time and its relative amplitude, respectively. β_i, ±0.02; θ_i, ±0.2 ns.

TABLE 5 Parameters from the fit of an associative model to the fluroescence anisotropy decay of *t*-PnA in large unilamellar vesicles of single lipids (DMPC, DPPC, POPC) and lipid mixtures of DMPC/DPPC

Sample	T/°C	θ_s/ns	r_∞^s	θ_f/ns	r_∞^f	χ^s	$\langle P_2\rangle^s$	χ^f	$\langle P_2\rangle^f$
DPPC	20	<0.1	0.34			1	0.94	0	
	30	<0.1	0.35			1	0.95	0	
	42	<0.1	0.30	0.5	0.11	0.17	0.88	0.83	0.53
	50			1.1	0.07	0		1	0.42
DMPC	15	<0.1	0.36			1	0.96	0	
	25	<0.1	0.34	1.4	0.13	0.20	0.94	0.80	0.58
	30			1.2	0.13	0		1	0.58
	40			0.3	0.11	0		1	0.53
DMPC/DPPC (1:1)	25	0.13	0.35			1	0.95	0	
	30	0.12	0.32			1	0.91	0	
	33	0.01	0.31			1	0.89	0	
	34	0.09	0.31	0.50	0.18	0.59	0.89	0.41	0.68
	35	0.19	0.32	0.47	0.18	0.30	0.91	0.70	0.68
	36	0.05	0.31	0.46	0.15	0.16	0.89	0.84	0.62
	37	<0.1	0.28	0.43	0.13	0.07	0.85	0.93	0.58
	38	0.05	0.26	0.47	0.14	0.04	0.82	0.96	0.58
	39	<0.1	0.26	0.51	0.11	0.01	0.82	0.99	0.53
	42			0.50	0.11	0		1	0.53
	45			0.67	0.10	0		1	0.51
DMPC/DPPC (7:3)	29	0.07	0.32			1	0.91	0	
	30	1.04	0.32			1	0.91	0	
	31	<0.1	0.31	0.44	0.12	0.35	0.89	0.65	0.55
	32	<0.1	0.29	0.80	0.13	0.09	0.86	0.91	0.56
	33	<0.1	0.28	0.65	0.13	0.04	0.85	0.96	0.59
	34	0.1	0.28	0.59	0.14	0.01	0.85	0.99	0.59

$\langle P_2\rangle^s$ and $\langle P_2\rangle^f$ are, respectively, the order parameters of the probe in the gel and fluid phases; χ^s and χ^f represent the lipid phase fraction derived from the parameters of the *t*-PnA fluorescence decay. θ_n, ±0.1 ns; r_∞, ±0.01.
Order parameters are calculated from $\langle P_2\rangle^2 = r_\infty/r_0$, with $r_0 = 0.39$ (Hudson and Cavalier, 1988).

to a decreasing in the polarizability of the solvents associated to the viscosity decreasing. Our experiments show that in simple alkane solvents the photophysical properties of *t*-PnA are preserved up to 490 cP in the temperature range between 10° and 50°C. At each temperature, a plot of log τ_L vs. log η shows a linear behavior in the range of viscosities studied (data not shown). Therefore, it is possible to estimate the viscosity of alkane solvents just from the *t*-PnA fluorescence lifetimes.

The time-resolved anisotropy measurements in paraffin oil indicate that the probe undergoes a complex rotational dynamics behavior. The three correlation times cannot be explained in terms of a symmetric ellipsoid rotating under the classic hydrodynamic principles. The variations of the longest and intermediate correlation times, θ_3 and θ_2, vs. T/η are linear (data not shown). If only these two correlation times are considered, the behavior with T/η could be interpreted by modeling the probe as a prolate ellipsoid of dimension 15 × 1 Å, where the absorption and emission transition moments are collinear and inclined 17° ± 2° in relation to the long axis of the molecule. The value obtained for the angle is in good agreement with the value of 20° recently determined using an oriented mixed crystal system in which the probe is oriented by inclusion in a urea/*n*-alkane inclusion complex (Shang et al., 1991). An independent determination of the orientation of the transition-dipole moment for tetraene chromophore of *t*-PnA was also made by analyzing the time-resolved fluorescence polarization of decatetraene in

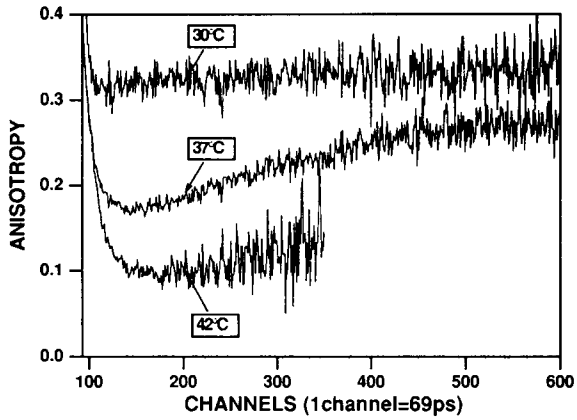

FIGURE 6 Time-resolved fluorescence anisotropy of *t*-PnA in large unilamellar vesicles of an equimolar mixture of DPPC/DMPC as a function of temperature (see Table 5 for parameters of decay).

paraffin oil (Dou et al., 1992). From this study, an angle of 22 ± 2° was obtained, which is also in good agreement with our result.

The shortest correlation time could be explained assuming fast movements of the chain as *trans-gauche* isomerization in the upper part of the molecule (Hudson et al., 1986). Comparing the correlation times in paraffin oil and cyclohexane with their respective viscosities, it is noticed that the rotational characteristics of the probe are different in both solvents. Since in paraffin oil solvent and probe present the same molecular size, it is possible that *t*-PnA does not displace the solvent molecules during its rotation (slip motion). However, the rotation of the probe in the cyclohexane must displace some solvent (due to the smaller molecular size of cyclohexane), and hence the free rotation of the probe will be partially damped (stick motion).

A wide variety of stable configurations can be assumed for *t*-PnA molecule. Contrary to DPH, the rotational behavior of this probe in isotropic solvents cannot be extrapolated to lipid bilayers environments. *t*-PnA remains anchored in the membrane by its acid group at the level of the phospholipid polar heads. This location prevent the molecule to adopt many configurations that are possible in isotropic solvents.

Lipid bilayers

The most important result of the analysis of the fluorescence kinetics of *t*-PnA in the fluid phase of a lipid bilayer is that the fluorescence lifetime distribution resembles that obtained in pure homogeneous solvents. Therefore it is possible to associate changes observed in this distribution pattern to changes in the physical state of the lipids. We are led to the conclusion that the rising of the third lifetime component observed at the transition temperature corresponds to the emission of the probe localized in the gel phase and its amplitude reflects the fraction of this phase.

In the fluid phase the temperature dependence of the long lifetime component decreases on going from DPPC to DMPC and from here to POPC. Activation energies determined for the three systems are, respectively, 12 ± 2, 8.4 ± 1.3, and 7.6 ± 0.3 kcal/mol, which are considerably higher than the value of 5.3 kcal/mol determined in paraffin oil. At 45°C, the respective order parameters of the probe is 0.53, 0.42, and 0.34. Therefore, the lifetime values of the probe and their temperature dependence are strongly dependent on the order of the system. In conclusion, lifetimes of *t*-PnA in fluid systems increase with order and viscosity and decrease with temperature. If the radiative lifetime of the probe is also constant in these systems, the radiationless process for *t*-PnA will be activated by increasing temperature and decreasing viscosity and order degree.

In contrast to that observed in DMPC and DPPC, the lifetime distribution of *t*-PnA in the fluid phase of POPC shows three lifetime components at low temperatures. This distribution pattern is similar to that observed in a gel phase, but it is centered to shorter lifetimes. At 10°C the order parameter in POPC is $\langle P_2 \rangle = 0.56$, which is in the same range that the value obtained in the fluid phase of DMPC. However, the longest lifetime of the distribution is 5 ns larger in the unsaturated phospholipid. The difference is due to the temperature dependence of the *t*-PnA radiationless decay rate (see above). This temperature dependence could also explain the origin of the intermediate lifetime in POPC: the fluorescent kinetics of the probe in a membrane system presents three lifetime components. The shortest lifetime component is almost independent of temperature, order, and fluidity. The intermediate and long lifetimes are extremely sensitive to these three parameters. At high temperatures, it is not possible to resolve the short and intermediate lifetimes, however, when order and viscosity increase with lowering temperature, these lifetimes can be resolved and the corresponding distribution pattern is described by three lifetimes components. Since the interpretation of data in terms of phase fractions is mainly lead by the amplitude of the longest lifetime, the presence of the intermediate lifetime does not interfere with the results (see companion paper (Mateo et al., 1993)).

It is known that *t*-PnA is dissolved preferentially in lipid environments with gel-like properties (Sklar et al., 1977b). This probe accumulates in the gel phase with a partition coefficient $K_p^{S/F} = 5 \pm 2$ (Sklar et al., 1977b; Hudson et al., 1986, 1988). From this value, combined with our experimental data, we have quantified (Eq. 17) the amount of the fluid and gel phase in the DMPC/DPPC mixture as a function of temperature. The results are given in Table 5. Since the radiative constants of *t*-PnA in each lipid phase can be considered similar (Sklar et al., 1977a), the fraction of the probe localized in the gel phase, χ_p^s, is determined from the relative proportion of the longest lifetime component (C_3 in Table 1 and 3). For this calculus it is assumed that $\chi_p^s = 1$ when C_3 reaches its maximum value. The DPPC/DMPC phase diagram determined from these data is shown in Fig. 7 together with the ideal and experimental phase diagram of Mabrey and Sturtevant (1976). In this diagram the beginning of the "lipid solidification" (*upper curve*) agrees well with that calculated assuming ideal mixing of the lipids, but it is detected at temperatures slightly higher than those of the calorimetric

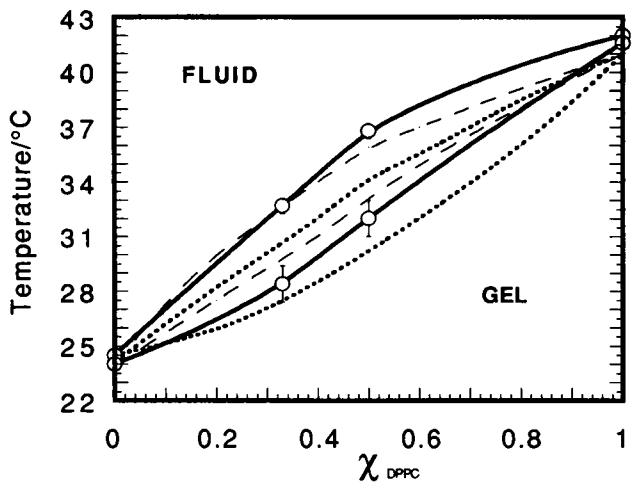

FIGURE 7 Thermotropic phase diagram of the DMPC/DPPC lipid mixture as determined from the *t*-PnA fluorescence lifetime distribution data (*solid lines*), from differential scanning calorimetry (*dotted lines*), and calculated assumming ideal mixing of the two lipids (*dashed lines*) (Mabrey and Sturtevant, 1976).

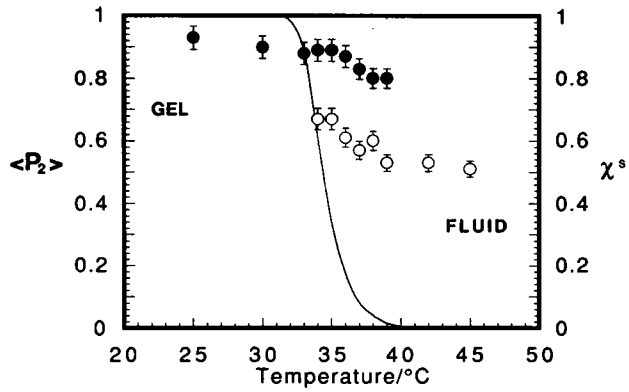

FIGURE 8 The order parameters of the fluid $\langle P_2 \rangle^f$ (○) and gel phase $\langle P_2 \rangle^s$ (●) of the DPPC/DMPC equimolar mixture as a function of temperature. The continuous line shows the variation with temperature of the fraction of gel phase χ^s.

results. This discrepancy can be explained because the calorimetric phase diagram was determined in multilamellar suspensions but not in large unilamellar vesicles. Another explanation could be the preference of the *t*-PnA for the gel phase. This preference makes it much more sensible to small gel clusters that cannot be detected by other techniques. For the same reason, the beginning of the lipid fluidification (*lower curve*) is detected by *t*-PnA with large uncertainty and at temperatures higher than those determined by calorimetry.

The reproducibility of these phase diagrams supported our conclusion about the origin of the longest lifetime component. This conclusion is also confirmed from the results of the anisotropy decay. At temperatures where fluid and gel phases coexist the long-lifetime component is associated with an environment having an order parameter $\langle P_2 \rangle^s$ that is rather consistent with a gel phase. The value of $\langle P_2 \rangle^f$ for the environment associated with the short lifetimes is consistently lower than $\langle P_2 \rangle^s$. The temperature dependence of $\langle P_2 \rangle^f$ and $\langle P_2 \rangle^s$ in the equimolar DMPC/DPPC mixture is shown in Fig. 8. The progressive ordering effect in the fluid phase as temperature decreased can be attributed to the increasing and, consequently, packing of the gel phase. From 25° to 35°C the $\langle P_2 \rangle^s$ value is practically constant. From 35° to 39°C, $\langle P_2 \rangle^s$ shows a smooth decrease. The discontinuity observed in $\langle P_2 \rangle^s$ at 35°C could be explained considering the connectivity property of domain systems (Vaz et al., 1989, 1990). In a two-components two-phase bilayer the phase rich in the major component has dispersed in it a discontinuous phase rich in the minor component. As temperature is increased, the initially dispersed phase becomes continuous, and the initial continuous phase becomes disperse. If the two components mix ideally, the connectivity will occur when the masses of the two coexisting phases are equal (Vaz et al., 1990). The binary system of DMPC/DPPC can be considered almost ideal. We have determined a $\chi^s = 0.5$ at 34.5°C in the equimolar mixture. Therefore, below this temperature the fluid phase is disconnected by a continuous gel phase. $\langle P_2 \rangle^s$ is similar to that observed in the pure gel phase, while $\langle P_2 \rangle^f$ is higher than the value expected for a fluid phase. At 34.5°C the fluid phase achieves the connectivity and gel clusters are dispersed in the bulk fluid phase. As the interaction between lipid clusters is screened by a boundary layer of lipid in intermediate states, $\langle P_2 \rangle^s$ decreases gradually with temperature and becomes smaller than the value expected for a pure gel phase.

Finally, in the contrary to the expected results, the experimental rotational correlation times are smaller in the gel than in the fluid phase. The value obtained in the fluid phase is probably the average of two depolarization processes: a fast motion, similar to the single one observed in the gel phase, along with another slower motion in the subnanosecond time range. The very fast depolarization of the probe in the ordered phase could be explained by *trans-gauche* isomerizations in the saturated part of the *t*-PnA chain, which could be more probable than motions of the entire acyl chain.

In conclusion, this work confirms that the fluorescence kinetics of *t*-PnA can be used to detect the presence of gel-fluid heterogeneity in lipid bilayers. In addition, we propose here a simple and very useful method to quantify and characterize this lateral heterogeneity using the fluorescence lifetime distribution of the probe incorporated in the bilayers. We believe that this method can be applied to a large variety of lipid membrane studies where the formation of heterogeneous microdomains is being postulated.

We thank Dr. Patrick Tauc of Laboratoire pour l'Utilisation du Rayonnement Electromagnétique for assistance with the picosecond laser and Dr. Fabienne Merola, who was in charge of the SA1 beam and the experimental set up.

The collaboration of Dr. Francisco Amat in the purification of the probe is gratefully acknowledge. We also acknowledge financial aid from an ECLURE grant and Dirección General de Investigación Cientifica y Técnica Project PB 90-0102. C. R. Mateo acknowledges the support of a fellowship from the Spanish Ministerio de Educación y Ciencia.

REFERENCES

Aloia, R. C., C. C. Curtain, and L. M. Gordon. 1988. Lipid domains and the relationship to membrane function. *In* Advances in Membrane Fluidity. R. C. Aloia, series editor. Vol. 2. Alan R. Liss, Inc, New York.

Barrow, D. A., and B. R. Lentz. 1985. Membrane structural domains. Resolution limits using diphenylhexatriene decay. *Biophys. J.* 48:221–234.

Brochon, J. C., and A. K. Livesey. 1988. Time-resolved fluorimetry using synchrotron radiation and maximum entropy method of analysis. *In* Light in Biology and Medicine. R. H. Douglas, J. Moan, and F. Dall'Acqua, editors. Plenum Publishing Corp. New York. 21–29.

Brochon, J. C., F. Merola, and A. K. Livesey. 1992. Time-resolved fluorescence study of dynamics parameters in biosystem. *In* Synchrotron Radiation and Dynamic Phenomena. Edited by the American Institute of Physics. New York. Vol. 258. 435–452.

Bultmann, T., W. L. C. Vaz, E. C. C. Melo, R. B. Sisk, and T. E. Thompson. 1991. Fluid-phase connectivity and translational diffusion in a eutectic two-component, two phase phosphatidylcholine bilayer. *Biochemistry.* 30:5573–5570.

Conti, F., and T. Parasassi. 1987. Lifetime of Fluorophores excited state in biological membranes and their model system. *In* Biophysics and Synchrotron Radiation. A. Bianconi and A. C. Castellano, editors. Springer-Verlag, Berlin Heidelberg. 328–333.

Cross, A. J., and G. R. Flemming. 1984. Analysis of time-resolved fluorescence anisotropy decays. *Biophys. J.* 46:45–56.

Davenport, L., J. R. Knutson, and L. Brand. 1988. Time-resolved fluorescence anisotropy of membrane probes: rotation gated by packing fluctuations. *In* Time Resolved Laser Spectroscopy in Biochemistry. J. R. Lackowicz, editor. *Proc. SPIE.* 909:263–270.

Devaux, P. H. and, M. Seigneuret. 1985. Specific of lipid protein interactions as determined by specytroscopic techniques. *Biochim. Biophys. Acta.* 822:63–125.

Dou, X., Q.-Y. Shang, and B. S. Hudson. 1992. Analysis of the decay of the fluorescence anisotropy of 2:4,6,8-decatetraene in a viscous hydrocarbon solution: the off-axis orientation of the transition dipole moment. *Chem. Phys. Lett.* 189:48–53.

Fiorini, R. M., M. Valentino, M. Glasser, E. Gratton, and G. Curatola. 1988. Fluorescence lifetime distributions of 1:6-diphenyl-1,3,5-hexatriene reveal the effect of cholesterol on the microheterogeneity of erythrocyte membrane. *Biochim. Biophys. Acta.* 939:485–492.

Gordon, L. H., P. W. Mobley, J. A. Esgate, G. Hoffman, A. D. Whetton, and M. D. Houslay. 1983. Thermotropic lipid phase separation in human platelet and rat liver plasma membrane. *J. Membr. Biol.* 76:139–149.

Ho, C., B. W. Williams, and C. D. Stubbs. 1992. Analysis of cell membrane micro-heterogeneity using the fluorescence lifetime of DPH-type fluorophores. *Biochim. Biophys. Acta.* 1104:273–282.

Hope, M. J., M. B. Bally, G. Webb, and P. R. Cullis. 1985. Production of large unilamellar vesicles by a rapid extrusion procedure. Characterisation of size distribution, trapped volume and ability to maintain a membrane potential. *Biochim. Biophys. Acta.* 812:55–65.

Hudson, B., and S. Cavalier. 1988. Studies of membrane dynamics and lipid-protein interactions with parinaric acid. *In* Spectroscopic membrane probes, Vol. 1. L. M. Loew, editor. CRC Press, Inc., Boca Raton. FL. 43–62.

Hudson, B. S., and B. E. Kohler. 1973. Polyene spectroscopy: the lowest energy excited singlet state of diphenyloctatetraene and other linear polyenes. *J. Chem. Phys.* 59:4984–5002.

Hudson, B. S., D. L. Harris, R. D. Ludescher, A. Ruggiero, A. Cooney-Freed, and S. A. Cavalier. 1986. Fluorescence probe studies of protein and membranes. *In* Aplications of fluorescence in the Biomedical Sciences. D. L. Taylor, A. S. Waggoner, F. Lanni, R. F. Murphy, and R. Birge, editors. Alan R. Liss, Inc., New York. 159–202.

Illsley, N. P., H. Y. Lin, and A. S. Verkman. 1988. Lipid phase structure in epithelial cell membranes: comparison of renal brush border and basolateral membranes. *Biochemistry.* 27:2077–2083.

Jaynes, E. T. 1983. Papers on probability, statistics and statistical physics. R. D. Rosenkrantz, editor. D. Reidel, Dordrecht, The Netherlands.

Lentz, B. R. 1989. Membrane "fluidity" as detected by diphenylhexatriene probes. 1989. *Chem. Phys. Lipids.* 50:171–190.

Livesey, A. K., and J. Skilling. 1985. Maximum entropy theory. *Acta Chrystallogr. Sect. B. Struct. Chrys. Chem.* A41:113–122.

Livesey, A. K., and J. C. Brochon. 1987. Analyzing the distribution of decay constants in pulse-fluorimetry using the maximum entropy method. *Biophys. J.* 52:693–706.

Ludescher, R. D., L. Peting, S. Hudson, and B. Hudson. 1987. Time-resolved fluorescence anisotropy for systems with lifetime and dynamic heterogeneity. *Biophys. Chem.* 28:59–75

Mabrey, S., and J. M. Sturtevant. 1976. Investigation of phase transitions of lipids mixtures by high sensitivity differential scanning calorimetry. *Proc. Natl. Acad. Sci. USA.* 73:3862–3866.

Mateo, C. R., M. P. Lillo, J. Gonzalez-Rodriguez, and A. U. Acuña. 1991. Lateral heterogeneity in human platelet plasma membrane and lipids from the time resolved fluorescence of *trans*-parinaric acid. *Eur. Biophys. J.* 20:53–59.

Mateo, C. R., P. Tauc, and J.-C. Brochon. 1993. Pressure effects on tyhe physical properties of lipid bilayers detected by *trans*-parinaric acid fluorescence decay. *Biophys. J.* 65:2248–2260.

Moya, I., M. Hodges, and J.-C. Barbet. 1986. Modification of room-temperature picosecond chorophyll fluorescence kinetics in green algae by photosystem II trap closure. *FEBS Lett.* 198:256–262.

Parasassi, T., F. Conti, and E. Gratton. 1984. Study of heterogeneous emission of parinaric acid isomers using multifrequency phase fluorometry. *Biochemistry.* 23:5660–5664.

Parasassi, T., G. De Stasio, A. D'Ubaldo, and E. Gratton. 1990. Phase Fluctuation in phospholipid membranes revealed by Laurdan fluorescence. *Biophys. J.* 57:1179–1186.

Parasassi, T., G. De Stasio, G. Ravagnan, R. M. Rush, and E. Gratton. 1991a. Quantitation of lipid phases in phospholipid vesicles by the generalized polarization of Laurdan fluorescence. *Biophys. J.* 60:179–189.

Parasassi, T., G. De Stasio, R. M. Rusch, and E. Gratton. 1991b. A photophysical model for diphenylhexatriene fluorescence decay in solvents, and in phospholipid vesicles. *Biophys. J.* 59:466–475.

Ruggiero, A., and B. Hudson. 1989a. Critical density fluctuations in lipid bilayers detected by fluorescence lifetime heterogeneity. *Biophys. J.* 55: 1111–1124.

Ruggiero, A., and B. Hudson. 1989b. Analysis of the anisotropy decay of trans-parinaric acid in lipid bilayers. *Biophys. J.* 55:1125–1135.

Schroeder, R. 1983. Lipid domains in plasma membranes from rat liver. *Eur. J. Biochem.* 132:509–516.

Shang, Q.-Y., X. Dou, and B. S. Hudson. 1991. Off-axis orientation of the electronic transition moment for a linear conjugated polyene. *Nature (Lond.).* 352:703–705.

Sklar, L. A., B. S. Hudson, M. Petersen, and J. Diamond. 1977a. Conjugated Polyene fatty acids on fluorescent probes: spectroscopic characterisation. *Biochemistry.* 16:813–818.

Sklar, L. A., B. S. Hudson, R. D. Simoni. 1977b. Conjugated polyene fatty acids as fluorescent probes: synthetic phospholipid membrane studies. *Biochemistry.* 16:819–828.

Van der Meer, B. W. 1988. Biomembrane structure and dynamics viewed by fluorescence. *In* Subcellular Biochemistry, Vol. 13. Fluorescence studies on Biological Membranes. H. J. Hilderson, editor. Plenum Press, New York. 1–53.

Van der Meer, B. W., H. Pottel, W. Herreman, M. Ameloot, and H. Hendrickx. 1984. Effect of orientational order on the decay of the fluorescence anisotropy in membrane suspension. *Biophys. J.* 46:515–523.

Vaz, W. L. C., E. C. C. Melo, and T. E. Thompson. 1989. Translational diffusion and fluid domain connectivity in a two-component, two phase phospholipid bilayer. *Biophys. J.* 56:869–876.

Vaz, W. L. C., E. C. C. Melo, and T. E. Thompson. 1990. Fluid phase connectivity in an isomorphus, two-component, two phase phosphatidylcholine bilayer. *Biophys. J.* 58:273–275.

Wolber, P. K., and B. S. Hudson. 1981. Fluorescence lifetime, and time-resolved polarization anisotropy studies of acyl chain order, and dynamics in lipid bilayer. *Biochemistry.* 20:2800–2810.